J Mater Sci: Mater Electron (2015) 26:7174–7182
DOI 10.1007/s10854-015-3342-3

Dual mode luminescence in rare earth (Er^{3+}/Ho^{3+}) doped ZnO nanoparticles fabricated by inclusive co precipitation technique

Rupali Das[1] · Naveen Khichar[1] · Santa Chawla[1]

Received: 31 March 2015 / Accepted: 6 June 2015 / Published online: 13 June 2015

Abstract Dual excitation properties have been introduced in ZnO nanoparticles (~10 nm) through lanthanide (Er^{3+}/Ho^{3+}) doping by inclusive co precipitation at room temperature. Monophasic hexagonal ZnO nanoparticles form hierarchical micro flowers as a consequence of lanthanide doping. The Stokes and anti Stokes emissions were investigated under UV (399 nm) and IR (980 nm) excitation. The down-conversion emission under band edge excitation is in the blue region and the up-conversion (UC) emission of lanthanide doped ZnO nanocrystals exhibit strong green and red fluorescence bands for ZnO:Er^{3+} and only green band for ZnO:Ho^{3+}. Post synthesis annealing further improves luminescence properties in ZnO:Er^{3+} that exhibits triple mode excitation of fluorescence under UV as well as IR wavelengths 980 and 1550 nm, also confirmed by confocal fluorescence mapping. The measured dependence of pump power on UC emission suggest that lanthanide doping in ZnO leads to frequency up-conversion emission via two to three photon absorption processes.

1 Introduction

The recent advances in rare earth (RE) lanthanide ion doped nanoparticles of insulators with up-conversion (UC) luminescence having potential application in wide areas including color displays, biomedical diagnostics, lasers and detectors, photovoltaics have been studied extensively [1–5]. A strong UC luminescence from β-NaGdF4:Yb/Er microcrystals was reported under the excitation of a 980 nm laser and its application to amorphous silicon solar cells with different UC layer structures were designed and studied leading to 6–10-fold enhancement in photocurrent [6]. Also a recent study yields the effect of the phase and doping concentration of $Yb3^{+}$ ions on the UC emission intensity of NaGdF4:$Yb3^{+}$, $Tm3^{+}$ nanoparticles [7]. Special interest lies in multifunctional semiconductors which can be made efficient light emitters with tailored light emitting properties with appropriate doping of lanthanide ions. Among semiconductors, excellent optical and electrical properties of ZnO nanocrystals with a direct band gap (3.37 eV) makes it a promising host material for both RE ions as well as transition-metal ions to obtain efficient luminescent properties for applications in photovoltaic, opto-electronic and magnetic memory devices [8–17]. However, intensive research focus has been made in down conversion (DC) luminescence properties [18–20] and very few work has been reported on UC luminescence of ZnO doped with RE dopants like Er^{3+}, Yb^{3+} and Ho^{3+} [21–23]. Recently, a large enhancement in up-conversion luminescence of ZnO nanocrystals codoped with Er^{3+} ions and varied concentrations of silver (Ag) nanoparticles was reported. The surface plasmon resonance of silver NPs as well as the energy transfer from silver NPs to Er^{3+} ions appreciably influenced the UC luminescence intensity in the visible regions of the codoped ZnO nanoparticles [24]. In our earlier work [25], dual mode luminescence has been reported in ZnO doped with RE ion emitters Er^{3+}, Ho^{3+} and also sensitizer Yb^{3+} where synthesis was done by high temperature solid state reaction method which is an established method for incorporating rare earth ions in a host phosphor lattice and the size of particles was in micro meters.

✉ Santa Chawla
santa@nplindia.org

[1] Luminescent Materials Group, CSIR-National Physical Laboratory, Dr. K.S. Krishnan Road, New Delhi 110012, India

In this paper, in contrast, we have presented results that show room temperature inclusive co precipitation method could be successfully employed to effectively dope rare earth ions Er^{3+}, Ho^{3+} into ZnO nanoparticles so that they show dual excitation up-conversion properties (980 and 1550 nm excitation) that is conventionally obtained in micron sized phosphors. The RE doped ZnO nanoparticles form interesting hierarchical morphology and exhibit dual excitation and dual emission properties under UV and IR excitation. A strong UC luminescence in both the red and green region of the visible spectrum was realized depending upon the rare earth dopant Er^{3+}/Ho^{3+} under the excitation of a 980 nm diode laser. The effective up-conversion luminescence in Er^{3+}/Ho^{3+} doped ZnO nanoparticles could be realized without added sensitizer Yb^{3+} ions. The experimental result clearly suggests that rare-earth Er^{3+} and Ho^{3+} doped ZnO nanoparticles displays dual mode luminescence under UV and IR (980 nm) excitation. Also, ZnO:Er^{3+} nanoparticles have exhibited triple mode excitation properties i.e., they are excitable under UV excitation, NIR excitation at 980 nm and IR excitation at 1550 nm. ZnO:Er^{3+} nanocrystals emit efficient green light under 1550 nm IR excitation. The work presents dual and triple mode excitation in RE doped ZnO nanoparticles synthesized at room temperature and is very important for nano science and nanotechnology.

2 Experiments

2.1 Material synthesis

Undoped ZnO and Er, Ho doped ZnO nanoparticles were synthesized by co-precipitation (CPP) method at room temperature. The dopant Er/Ho (2 mol%) ions were included into the ZnO matrix by substitution in the crystal lattice in zinc position. For synthesizing undoped ZnO, sub molar (0.027 M) aqueous solution of zinc acetate was used as a precursor material. For RE (Er/Ho) doping, Zinc acetate (Zn $[(CH)_3\ (COOH)]_2{\cdot}2H_2O$) stock solution and sub molar aqueous Erbium nitrate ($Er(NO_3)_3$)/Holmium nitrate ($Ho(NO_3)_3$) solution were mixed under continuous magnetic stirring to make a homogeneous ensemble. Precipitation of nanoparticles was facilitated in an alkaline medium (pH = 10) by adding double diluted aqueous ammonia solution and stirring vigorously for 1 h followed by storage in preheated oven at 90 °C for 24 h. The precipitated nanoparticles were collected by decanting the clear top solution followed by cleaning ultrasonically with ethanol few times to remove all surface bound water that may act as luminescence quencher. The resulting material was dried in oven. CPP technique was chosen as it can effectively incorporate dopants with improved chemically homogeneity to prepare nano-sized particles. A part of ZnO:Er^{3+} powder sample was further annealed at 800 °C in air atmosphere for 2 h to investigate the effect of annealing on luminescence properties. Annealed sample was dispersed in PVA solution and drop casted on a microscope cover slip for confocal fluorescence studies.

2.2 Characterization

The crystalline phase of the synthesized samples were identified by the X-ray powder diffraction (XRD) using a Rigaku miniflex X-ray diffractometer using the principle of Bragg–Brentano Geometry. The XRD patterns were obtained with monochromatic Cu-Kα irradiation (1.54A°) with the diffraction angle 2θ scanned in the 20°–80° range.

The morphology of the undoped and Lanthanum doped ZnO powder samples were studied using a digital LEO 440 PC scanning electron microscope (SEM) and FEI TECNAI F 30 TWIN, TECNAI Transmission electron microscope (TEM). The photoluminescence (PL) excitation and emission spectra were recorded using combined steady state fluorescence and lifetime spectrometer of Edinburgh Instruments FLSP920 with Xe lamp as excitation source to obtain down conversion spectra of the samples. The up conversion photo luminescence spectra were acquired by exciting the powder samples with a power tunable 980 nm diode laser (MDL-N-980-6 W) coupled with optical fiber. The confocal fluorescence mapping and spectroscopy were carried out using a WITec Confocal fluorescence microscope (WITec 300 M^+) under successive excitation of three diode lasers with wavelengths 375, 980 and 1550 nm for studying thin film (drop casted). A specific area of the sample was studied under a 100× objective (NA 0.9) in the confocal microscope so that both DC and UC fluorescence distribution could be ascertained under excitation of UV (375 nm, 10 mW) and IR diode lasers (980 nm, 300 mW and 1550 nm, 8 mW). The fluorescence emission spectra was recorded using a high throughput lens based spectrograph (ACTON SP2300i) with 300 mm focal length, connected with a thermoelectrically cooled front illuminated CCD camera (ANDOR iVACDR324B-F1-354 with 1650 × 200 active pixels, with NIR enhanced F1 sensor). For the selected area (25 μm × 25 μm) fluorescence mapping, 150 points per line and 150 lines per image was used with integration time 0.1 s.

3 Results and discussion

3.1 Phase characterization

X-ray diffraction was used for phase characterization of as synthesized nanoparticles. All samples (undoped and

lanthanum doped) exhibited the three main peaks (100), (002) and (101) corresponding to "wurtzite hexagonal" phase of ZnO (JCPDS Card No. 36-1451) (Fig. 1) with varying intensities. The diffraction spectra of ZnO, ZnO:Er, ZnO:Ho synthesized by CPP method is monophasic and could be indexed to the "wurtzite hexagonal" phase of ZnO without any precipitated phase corresponding lanthanide oxide. The sharp diffraction peaks corresponding to ZnO in all samples indicate well crystalline structure and suggest that doping does not alter its wurtzite structure. The reduced peak intensities of the doped samples point to the decreased crystallinity of ZnO phase due to substitutional doping by lanthanum ions in ZnO lattice. Comparison of the diffraction angle for the doped and pure samples (Fig. 1) shows a peak shift which is related to the change in lattices parameters due to doping of larger lanthanide ion e.g., Er^{3+}(effective ionic radii 0.103 nm), Ho^{3+}(effective ionic radii 0.104 nm) in place of Zn^{2+} (effective ionic radii 0.088 nm). The effect of dopant on the crystalline parameters resulting in peak shift as calculated from the XRD data implies successful incorporation of the lanthanide ions into the ZnO crystals. However, effective substitution of Er^{3+}/Ho^{3+} in place of Zn^{2+} ions would introduce lattice strain due to accommodation of larger ionic radii trivalent rare earth ions resulting in change of lattice parameters as indicated in Table 1. Post synthesis annealing improves crystallinity and lattice parameters conform more to ZnO lattice. The average crystallite size in 'a' and 'c' directions, calculated using Scherer formula, for different doping of Er, Ho in ZnO varied from 32 to 51 nm.

For effective substitution of trivalent rare earth ion in place of divalent Zn ion, overall charge compensation in the ZnO lattice would require incorporation of two Er^{3+}(or Ho^{3+}) ions for three Zn^{2+} ions [25–28]. Further, for trivalent state of Er^{3+} dopant the overall charge neutrality in the lattice is sustainable, either by creating one Zn^{2+}

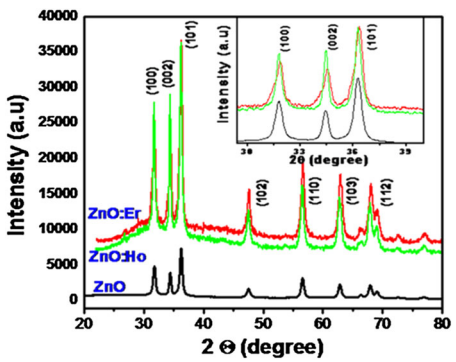

Fig. 1 XRD spectra of undoped and rare earth doped ZnO nanocrystals, *inset* shows the individual peaks with discernible peak shift due to doping

Table 1 Crystalline parameters along different planes of sample prepared by co-precipitation method

Sample	d (A°)	hkl	a = b ≠ c crystallite parameters (A°)
Undoped ZnO	2.813	100	a = 3.2486
	2.602	002	c = 5.2039
ZnO:Er^{3+}	2.597	100	a = 2.9988
	2.615	002	c = 5.2305
ZnO:Ho^{3+}	2.812	100	a = 3.2469
	2.603	002	c = 5.2053

vacancy for incorporation of each two Er^{3+} ions or introducing one oxygen interstitial (O_i^{2-}) defect in the following manner:

$$3Zn^{2+} = 2Er_{Zn}^{3+} + V_{Zn}^{2+}$$

or

$$3Zn^{2+} = 2Er_{Zn}^{3+} + Zn^{2+} + O_i^{2-}$$

But the formation probability of interstitial oxygen centres (O_i) is lesser due to bigger size of oxygen atoms whereas both the point defects V_{zn} (0.3 eV above valence band) and O_i (1.08 eV above the valence band) act as acceptor centres in ZnO lattice. As the XRD peak shift and change in lattice parameters due to doping of rare earth ions is not substantial (Table 1), particularly for Ho^{3+}, distribution of rare earth ion may involve both substitutional as well as interstitial RE^{3+} ions in ZnO lattice.

3.2 Morphology

The SEM micrographs show strikingly varied morphology of the pure ZnO nanoparticles in comparison to the lanthanide doped ZnO nanoparticles synthesized by CPP method (Fig. 2). The undoped ZnO exhibited spherical grains (5–10 nm) while all the lanthanum doped ZnO samples exhibit formation of micron sized flowers (Fig. 2). Doping with rare earth elements caused the grains to merge into a hierarchical formation of flower like structures with dimensions of around 2 μm for ZnO:Er^{3+} (Fig. 2b), and multi petalled bigger flowers (∼8μm) for ZnO:Ho^{3+} (Fig. 2c). Since, all the samples were prepared under identical synthesis conditions; these morphological changes could only be attributed to the strain induced in the lattice by substitutional doping of larger lanthanum ions. Dopant induced morphology change in ZnO particles have also been found with different dopants and synthesis conditions [27, 28].

The TEM images of a representative sample (ZnO:Er^{3+}) under different magnifications show that individual nanoflowers (2 μm) are formed by ensemble of nanoparticles of few nanometer dimension. The HRTEM imaging

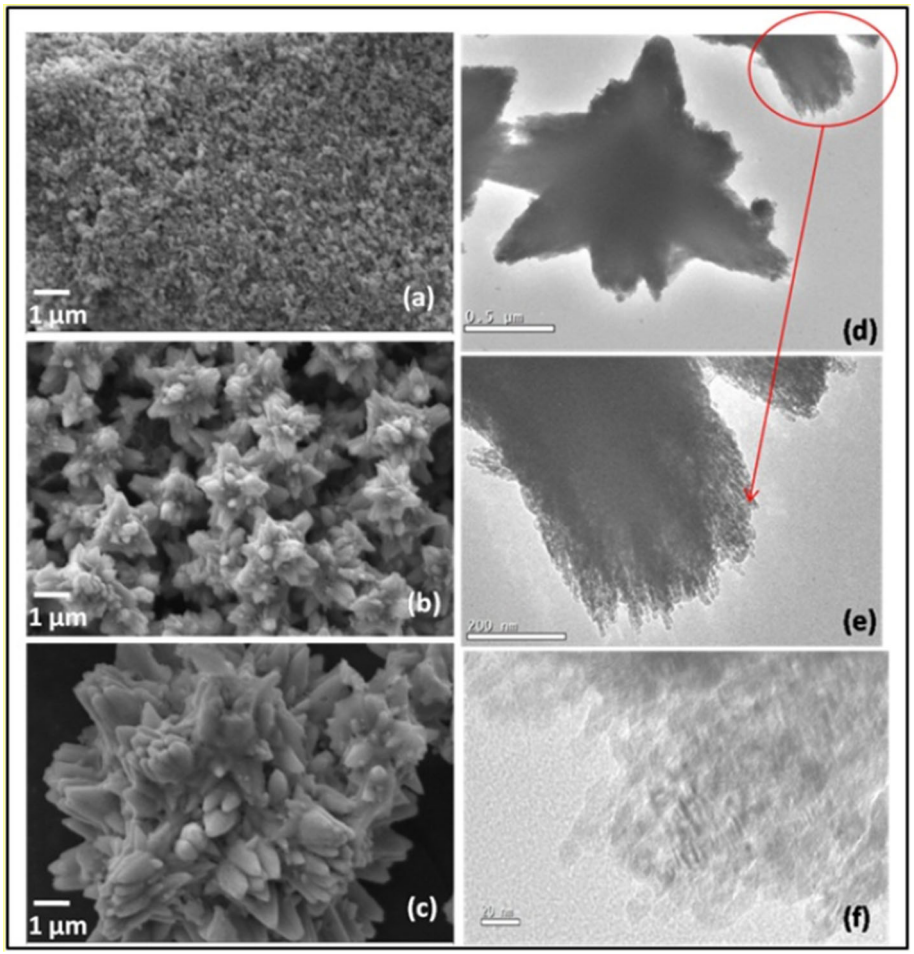

Fig. 2 SEM images of **a** undoped ZnO, **b** ZnO:Er^{3+}, **c** ZnO:Ho^{3+}. TEM images of ZnO:Er^{3+} with different magnifications (**d**) to (**f**) clearly show that individual nanoflowers of about 2 μm are hierarchically formed from ensemble of nanoparticles of few nanometer dimension

of ZnO:Ho^{3+} samples revealed similar patterns which indicate that individual nanoflowers/grains are formed by the ensemble of numerous nanoparticles and the morphology of the hierarchical flowers are affected by properties of the dopant.

3.3 Down conversion luminescence

The photoluminescence (PL) emission spectra of ZnO and ZnO:Er^{3+}/Ho^{3+} nanophosphor under UV excitation is shown in Fig. 3b corresponding to the peak excitation wavelength 399 nm as shown in the PL excitation spectra (Fig. 3a). The emission spectra for undoped ZnO show three peaks in the blue green region, the emission intensity, however decreases for RE doped samples. The actual photograph of the powder samples under UV excitation is shown in the inset of Fig. 3b. In ZnO samples synthesized in oxygen rich atmosphere, creation of zinc vacancies is favorable due to their low formation energy. The zinc vacancy centre (V_{Zn}) lie 0.3 eV above ZnO valence band and forms an acceptor centre [29]. Electrons in different intrinsic donor level can recombine with holes trapped in V_{Zn} acceptor centre to give rise to blue green emission peaks in undoped ZnO. Doping of rare earth ions changes the defect distribution due to change in local charge environment of larger trivalent ions, some of which may occupy interstitial position in near room temperature synthesis.

3.4 Up conversion luminescence

The upconversion photoluminescence emission spectra of rare earth doped ZnO samples under different excitation laser (980 nm) power are shown in Fig. 4. The effective substitution of bright RE emitters introduces the observed up-conversion luminescence from ZnO, which otherwise is not possible in undoped ZnO since photoluminescence is a very sensitive indicator of rare earth dopant ions. For the ZnO:Er^{3+} nanoparticles two distinct bands are observed in the red and green visible regions (Fig. 4a). The green emission dominates the spectra exhibiting distinct bands centered at 535 and 559 nm and the red one at 657 nm. The bright green emission bands can be assigned to $^4F_{7/2}$–$^4I_{15/2}$, $^2H_{11/2}$–$^4I_{15/2}$, $^4S_{3/2}$–$^4I_{15/2}$ and red emission from $^4F_{9/2}$–$^4I_{15/2}$

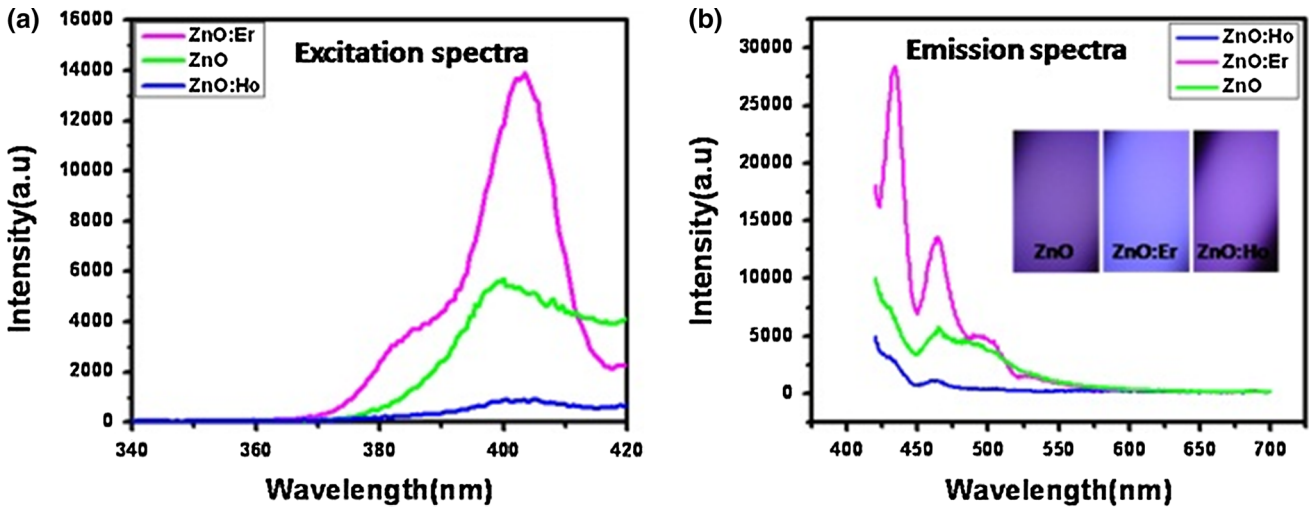

Fig. 3 Downconversion emission spectra under UV excitation of undoped Er^{3+} and Ho^{3+} lanthanide doped ZnO samples

transitions respectively. The UC spectra of ZnO:Er^{3+} on annealing to a temperature of about ~800 °C shown in Fig. 4b further shows distinctive up-converted luminescent emission band at 520, 549, 560 nm green region and 659 nm red peak with an enhancements in the red emission spectra. Further, the anti-Stokes luminescence was enhanced on annealing the as prepared sample as can be clearly discerned in Fig. 4d. The figure clearly shows that the green to red emission ratio is reversed upon annealing the sample which suggests a change in charge distribution among emitting Er^{3+} levels due to proper substitutional doping aided by annealing process and consequent change in phonon assisted relaxation process. The UC spectra of ZnO:Ho^{3+} sample further yields a change in the ratio of red and green emission. The UC emission yield from ZnO:Ho^{3+} sample is comparatively less from ZnO:Er^{3+} samples and the emission is predominantly in the green region centred at 524 and 553 nm with transitions from $^5S_2$, $^5F4$–$^5I_8$ whereas no appreciable red emission is observed. The dependence of UC emission intensity (I_{UC}) on the pumping IR laser power (I_i) was further quantified to better understand the mechanism of absorption of multiple low energy (IR) photons and UC emission of higher energy photon (visible) in the nanocrystalline phosphor material. The dependence follows a power law represented by $I_{UC} \propto I_i^n$. Also the non radiative multiphonon relaxation rate governs the upconversion emission efficiency depending upon the host lattice. Since ZnO is an oxide semiconductor with low phonon energy (440 cm^{-1}) corresponding to Zn–O vibrational bond [30], relaxation of excited lanthanide ions to ground state by emitting photons rather than phonons have more probability. A logarithmic plot of the integrated UC emission intensity as a function of the IR laser excitation power further elucidates the multiple photon absorption process in lanthanide RE ion doped ZnO as shown in the insets of each UC PL spectra (Fig. 4a–c). Fitting the data yields a straight line with ZnO:Er^{3+} samples displaying respective slope of 3.1 for red emission and 2.8 for green emission. For the ZnO:Er^{3+} annealed sample the red emission slope value is 2.7 and green emission slope is 2.8. For ZnO:Ho^{3+} sample, the slope value is 1.5 for green emission regions. The obtained power pump plots give a clear indication that the obtained up-conversion emissions in ZnO:Er^{3+} nanoparticles can be attributed to three photon processes and in ZnO:Ho^{3+} to two photon process.

3.5 Triple excitation properties of ZnO:Er^{3+}

As ZnO can be excited by UV light and emit in broad band and the level spacing of Er^{3+} ion $^4I_{15/2}$–$^4I_{11/2}$ correspond to 980 nm and $^4I_{15/2}$–$^4I_{13/2}$ to 1550 nm, triple excitation luminescence properties of ZnO:Er^{3+} (annealed sample, drop caste film on a microscope cover slip) was investigated under a confocal fluorescence microscope. The confocal fluorescence images of selected area under 375, 980 and 1550 nm diode laser are shown in Fig. 5a–c and corresponding emission spectra are shown in Fig. 5d–f respectively. The actual video images of drop casted film under 375 and 980 nm excitation laser are shown in the insets of Fig. 5d, e respectively that clearly shows the emission color commensurate with the spectra.

Upon UV excitation (375 nm), excitation of charge carriers across band gap and redistribution in intrinsic defect states give rise to broad emission, also a characteristic red emission from RE Er^{3+} ion corresponding to $^4F_{9/2}$–$^4I_{15/2}$ transition is clearly discernible in the confocal fluorescence spectra (Fig. 5d). Doping trivalent RE ions substitutionally

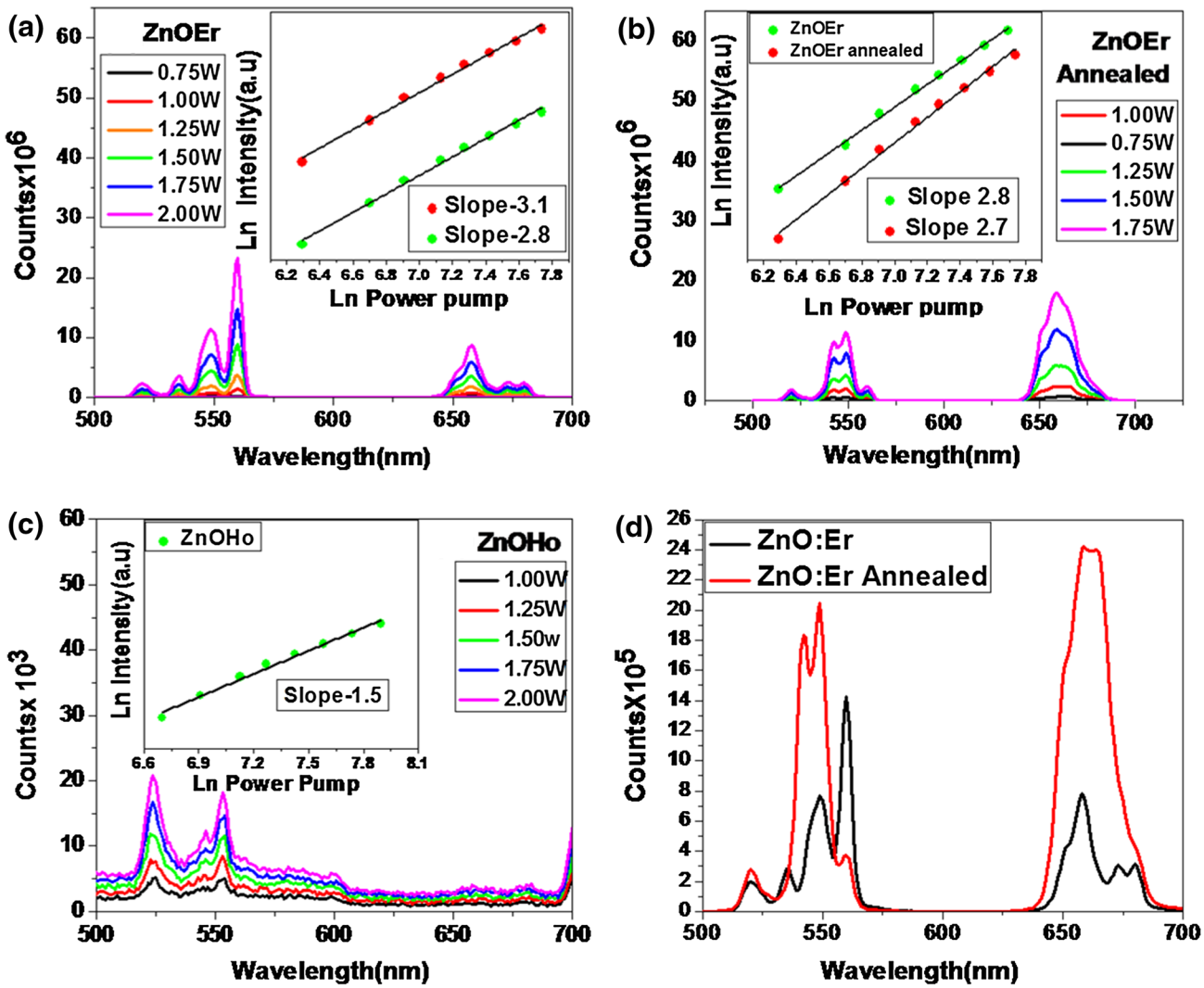

Fig. 4 Up conversion PL spectra of ZnO:Er^{3+}, annealed ZnO:Er^{3+}, ZnO:Ho^{3+} and a comparison of ZnO:Er^{3+} with the annealed sample respectively. The *inset* shows the dependence of UC intensity with pump power of the *green* and *red* emission (Color figure online)

in place of divalent zinc would require that two Er^{3+} ions are substituted for three Zn^{2+} ions. For maintaining overall charge neutrality in the lattice, either one Zn^{2+} vacancy need to be created for incorporation of each two Er^{3+} ions or one oxygen interstitial (O_i^{2-}) defect be introduced. Recombination of electrons from an intrinsic donor levels to V_{Zn} acceptor centre give rise to blue emission peaks. In addition, excited Er^{3+} ions can relax to ground state ($^4I_{15/2}$) giving rise to sharp red emission peak.

Confocal fluorescence spectra under 980 and 1550 nm IR laser illumination of (Fig. 5e, f) clearly show that the up-conversion photoluminescence occurs at both the wavelengths of excitation [30–32]. This happens due to direct excitation of Er^{3+} ions from $^4I_{15/2}$–$^4I_{11/2}$ level and $^4I_{15/2}$–$^4I_{13/2}$ level respectively through multiphoton absorption and population of upper Er^{3+} levels. The emission under 980 nm excitation comprise both green and red emission resulting in green yellow fluorescent colour (inset, Fig. 5e), the UC emission under 1550 nm excitation is dominantly red. Thus triple mode fluorescence characteristic of ZnO:Er^{3+} nanocrystals of average dimension 5–10 nm that form hierarchical nano flowers, is clearly established.

3.6 Energy level diagram

The energy level diagram (Fig. 6) elucidates the excitation and emission processes for both down and up conversion luminescence in rare earth (Er^{3+}, Ho^{3+}) ion doped ZnO. Upon UV excitation, electrons from valence band are excited across the band gap to the conduction band and can get redistributed to various donor levels, subsequent

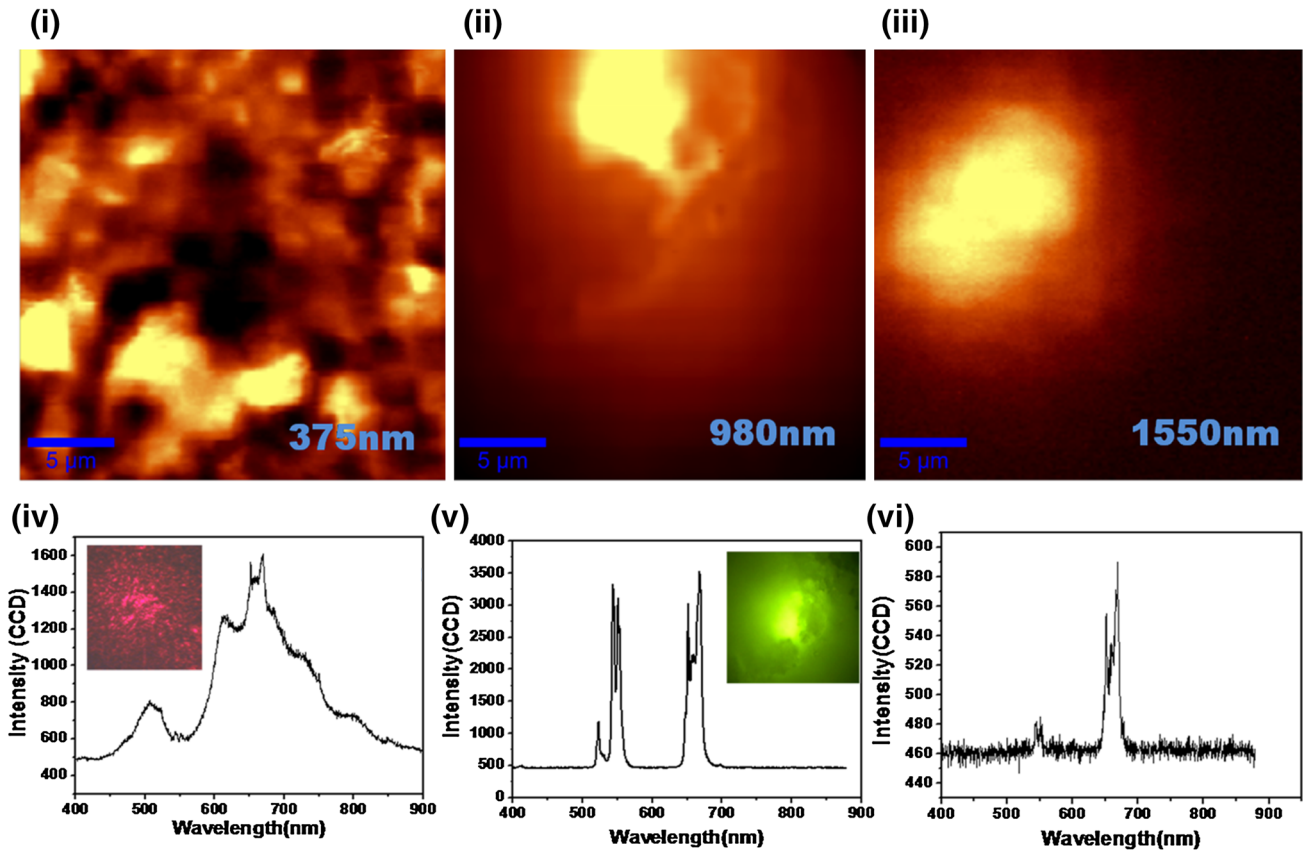

Fig. 5 Confocal fluorescence map and corresponding spectra of ZnO:Er^{3+} (annealed) under 375 nm UV excitation (**a**, **d**); under 980 nm IR excitation (**b**, **e**) and under 1550 nm IR excitation (**c**, **f**) respectively. The *insets* in (**d**) & (**e**) show the actual video image of drop casted film under 375 and 980 nm excitation laser

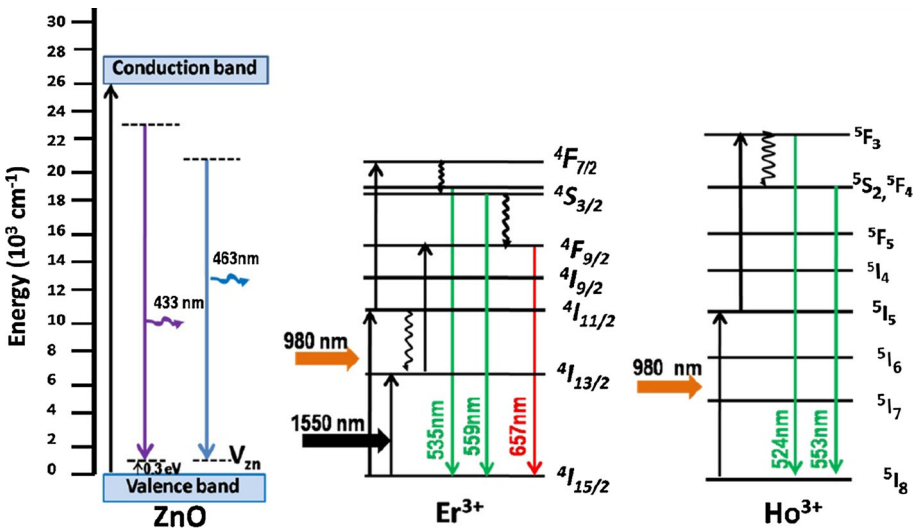

Fig. 6 Schematic energy level diagram, showing the DC and UC mechanisms in ZnO nanoparticles doped with Er^{3+}, Ho^{3+} under UV, 980 and 1550 nm excitation respectively

radiative recombination with holes at the acceptor centre (V_{Zn}) produce luminescence emission in blue region.

IR (980 nm) light, can directly excite RE ions (Er^{3+} and Ho^{3+}) from their respective ground states to various excited levels e.g., $^4I_{15/2}$–$^4I_{11/2}$ (Er^{3+}) and $^5I_8$–$^5I_5$ (Ho^{3+}). Upper emitting levels get occupied through multiphoton absorption through processes such as Excited State Absorption (ESA) or Energy Transfer (ET) and non radiative phonon assisted relaxation processes as shown in Fig. 6. The radiative recombination from upper excited

levels to ground state giving rise to characteristic emissions is depicted in Fig. 6. For Er^{3+} doped ZnO, when the red emission is dominant from the $^4F_{9/2}$ level, the population in that level is high due to ground state absorption from $^4I_{15/2}$ level, excited state absorption from $^4I_{11/2}$ and some multi phonon relaxation between $^4S_{3/2}$–$^4F_{9/2}$ levels. For 1550 nm emission in Er^{3+} doped ZnO, ground state excitation is between $^4I_{15/2}$–$^4I_{13/2}$ levels followed by similar process as above.

In Ho^{3+} system, the dominant green emission occurs when Ho^{3+} ions in the $^5S_2$, $^5F_4$ levels can relax to ground state $^5I_8$ by emission of green photons. The UC is two photon processes, and little red emission that could arise due to $^5F_5$–$^5I_8$ transition, is because of low non radiative relaxation probability from $^5S_2$, $^5F_4$ level to lower $^5F_5$ level in the as synthesized nanoparticles. Such two photon UC process in ZnO:Ho^{3+} (slope $\sim$ 1.6) has also been reported [25].

4 Conclusion

A room temperature co precipitation technique has been effectively employed to dope trivalent light emitters Er^{3+}/Ho^{3+} in ZnO lattice. RE doping changes the morphology to hierarchical micro flowers made of nanometer ($\sim$10 nm) sized particles and making them dual/triple excitation nanophosphor. Intrinsic ZnO synthesized in identical conditions under UV excitation yield blue fluorescence whereas doping with Er^{3+}/Ho^{3+} also makes them efficient up-conversion emitters when excited by IR light with emission peaks in green and red. ZnO:Er^{3+} nanoparticles exhibit triple mode luminescence, being simultaneously excitable by UV, 980 and 1550 nm IR light. The results conclusively show that ZnO nanoparticles can act as dual/triple excitation phosphor at the same time with tunable emission color by doping trivalent rare earth ions and can be potential light emitters/spectral converters.

Acknowledgments This present work was supported by the TAPSUN project under CSIR Solar Mission program of India.

References

1. S. Heer, K. Kompe, H. Gudel, M. Haase, Highly efficient multicolour upconversion emission in transparent colloids of lanthanide-doped $NaYF_4$ nanocrystals. Adv. Mater. **16**(23–24), 2102–2105 (2004). doi:10.1002/adma.200400772
2. F. Vetrone, J.C. Boyer, J.A. Capobianco, A. Speghini, M. Bettinelli, Concentration-dependent near-infrared to visible upconversion in nanocrystalline and bulk Y_2O_3:Er^{3+}. Chem. Mater. **15**(14), 2737–2743 (2003). doi:10.1021/cm0301930
3. G.S. Yi, H.C. Lu, S.Y. Zhao, G. Yue, W.J. Yang, D.P. Chen, L.H. Guo, Synthesis, characterization, and biological application of size-controlled nanocrystalline NaYF4:Yb, Er infrared-to-visible up-conversion phosphors. Nano Lett. **4**(11), 2191–2196 (2004). doi:10.1021/nl048680h
4. L. Wang, R.X. Yan, Z.Y. Hao, L. Wang, J.H. Zeng, J. Bao, X. Wang, Q. Peng, Y.D. Li, Fluorescence resonant energy transfer biosensor based on upconversion-luminescent nanoparticles. Angew. Chem. Int. Ed. **44**(37), 6054–6057 (2005). doi:10.1002/anie.200501907
5. W. Chen, J.Z. Zhang, A.J. Joly, Optical properties and potential applications of doped semiconductor nanoparticles. J. Nanosci. Nanotechnol. **4**(8), 919–947 (2004). doi:10.1166/jnn.2004.142
6. R. Cheng, Y. Chen, Z. Li, X. Chen, P. Yang, H. Zhu, Y. Huang, Z. Sun, S. Huang, Citric acid-assisted growth of lanthanide ions co-doped one-dimensional upconversion microcrystals and their photovoltaic applications. J. Mater. Sci.: Mater. Electron. **25**, 4066–4073 (2014). doi:10.1007/s10854-014-2130-9
7. Y. Miao, P. Wang, H. Guan1, and Y. Chen, Synthesis and up-conversion luminescence of NaGdF4:$Yb3^+$, $Tm3^+$. J Mater Sci. Mater Electron (2015). doi:10.1007/s10854-015-3132-y
8. A. Gupta, A.D. Compaan, All-sputtered thin-film solar cell with transparent conducting oxide. Appl. Phys. Lett. **85**, 684–686 (2004). doi:10.1063/1.1775289
9. Z.L. Wang, Functional oxide nanobelts: materials, properties and potential applications in nanosystems and biotechnology. Annu. Rev. Phys. Chem. **55**, 159–196 (2004). doi:10.1146/annurev.physchem.55.091602.094416
10. C.S. Rout, A.R. Raju, A. Govindaraj, C.N.R. Rao, Hydrogen sensors based on ZnO nanoparticles. Solid. State. Commun. **138**(3), 136–138 (2006). doi:10.1016/j.ssc.2006.02.016
11. Z.L. Wang, C.K. Lin, X.M. Liu, Y. Luo, Z.W. Quan, H.P. Xiang, L. Lin, tunable photoluminescent and cathodoluminescent properties of ZnO and ZnO:Zn phosphors. J. Phys. Chem. B. **110**(19), 9469–9476 (2006). doi:10.1021/jp057214t
12. G. Seisenberger, M.U. Ried, T. Endress, H. Buning, M. Hallek, C. Brauchle, Real-time Sin 31f0 gle-molecule imaging of the infection pathway of an adeno-associated virus. Science **294**, 1929 (2001). doi:10.1126/science.1064103
13. J.M. Daewas, P. Dekker, P. Burns, J.A. Piper, Self-frequency-doubling ytterbium lasers. Opt. Rev. **12**, 101–104 (2005). doi:10.1007/s10043-004-0101-8
14. G.S. Yi, B.Q. Sun, F.Z. Yang, D.P. Chen, Y.X. Zhou, J. Cheng, Synthesis and characterization of high-efficiency nanocrystal up-conversion phosphors: ytterbium and erbium codoped lanthanum molybdate. Chem. Mater. **14**(7), 2910–2914 (2002). doi:10.1021/cm0115416
15. M.U. Staudt, S.R. Hastings-Simon, M. Nilsson, M. Afzelius, V. Scarani, R. Ricken, H. Suche, W. Sohler, W. Tittel, N. Gisin, Fidelity of an optical memory based on stimulated photon echoes. Phys. Rev. Lett. **98**, 113601–113604 (2007). doi:10.1103/PhysRevLett.98.113601
16. H. Desirena, E. De la Rosa, A.L. Diaz-Torres, A.G. Kumar, Concentration effect of Er^{3+} ion on the spectroscopic properties of $Er^{3+}$and Yb^{3+}/Er^{3+} co-doped phosphate glasses. Opt. Mater. **28**(5), 560–568 (2006). doi:10.1016/j.optmat.2005.04.002
17. F. Gu, S.F. Wang, M.K. Lu, G.J. Zhou, D. Xu, D.R. Yuan, Structure evaluation and highly enhanced luminescence of Dy^{3+}-Doped ZnO nanocrystals by Li^+ doping via combustion method. Langmuir **20**(9), 3528–3531 (2004). doi:10.1021/la049874f
18. A. Ishizumi, Y. Kanemitsu, Structural and luminescence properties of Eu-doped ZnO nanorods fabricated by a microemulsion method. App. Phys. Lett. **86**, 253106–253108 (2005). doi:10.1063/1.1952576
19. J. Wang, M.J. Zhou, S.K. Harik, Q. Li, D. Tang, M.W. Chu, C.H. Chen, Local electronic structure and luminescence properties of Er doped ZnO nanowires. Appl. Phys. Lett. **89**, 221917–221919 (2006). doi:10.1063/1.2399340
20. A.S. Pereira, M. Peres, M.J. Soares, E. Alves, A. Neves, T. Monteiro, T. Trindade, Synthesis, surface modification and

optical properties of Tb3 + -doped ZnO nanocrystals. Nanotechnology **17**(3), 834 (2006). doi:10.1088/0957-4484/17/3/037
21. Y. Liu, Q. Yang, C. Xu, Single-narrow-band red upconversion fluorescence of ZnO nanocrystals codoped with Er and Yb and its achieving mechanism. J. Appl. Phys. **104**, 064701–064705 (2008). doi:10.1063/1.2980326
22. X. Wang, X. Kong, G. Shan, Y. Yu,Y. Sun, L. Feng, K. Chao, S. Lu, Y. Li, Luminescence spectroscopy and visible upconversion properties of Er3+ in ZnO nanocrystals. J. Phys. Chem. B. **108**(48), 18408–18413 (2004). doi:10.1021/jp048021t
23. Y. Bai, Y. Wang, K. Yang, X. Zhang, Y. Song, C.H. Wang, Enhanced upconverted photoluminescence in Er3 + and Yb3 + codoped ZnO nanocrystals with and without Li^{+} ions. Opt. Commun. **281**(21), 5448–5454 (2008). doi:10.1016/j.optcom.2008.07.041
24. J. Yang, H. Zhang, X. Wang, F. Qin, C. Wang, Optical properties of Er^{3+}–Ag co-doped ZnO nanocrystals prepared by combustions method. J. Mater. Sci. Mater. Electron. **25**, 3895–3900 (2014). doi:10.1007/s10854-014-2104-y
25. N. Kichar, S. Bishnoi, S. Chawla, Introducing dual excitation and tunable dual emission in ZnO through selective lanthanide (Er^{3+}/Ho^{3+}) doping. RSC Adv. **4**, 18811–18817 (2014). doi:10.1039/C4RA01248H
26. A. Pawar, A. Jadhav, C.W. Kim, H.G. Cha, U. Pal, Y.S. Kang, Emission controlled dual emitting Eu-doped $CaMgSi_2O_6$ -nanophosphors. J. Lumin. **157**, 131–136 (2015). doi:10.1016/j.jlumin.2014.08.034
27. K. Jayanthi, S. Chawla, K.N. Sood, M.S. Chhibara Singh, Dopant induced morphology changes in ZnO nanocrystals. Appl. Surf. Sci. **255**(11), 5869–5875 (2009). doi:10.1016/j.apsusc.2009.01.032
28. K. Jayanthi, S. Chawla, A. Joshi, Z.H. Khan, R.K. Kotnala, Fabrication of luminescent, magnetic hollow core nanospheres and nanotubes of Cr-Doped ZnO by inclusive coprecipitation method. J. Phys. Chem. C. **114**, 18429–18434 (2010). doi:10.1021/jp107086h
29. B. Lin, Z. Fu, Y. Jia, Green luminescent center in undoped zinc oxide films deposited on silicon substrates. Appl. Phys. Lett. **79**, 943–945 (2001). doi:10.1063/1.1394173
30. F. Vetrone, J.C. Boyer, J.A. Capobianco, A. Speghini, M. Bettineli, 980 nm excited upconversion in an Er-doped ZnO–TeO_2 glass. Appl. Phys. Lett. **80**, 1752–1754 (2002). doi:10.1063/1.1458073
31. G.A. Kumar, M. Pokhrel, D.K. Sarda, Intense visible and near infrared upconversion in M_2O_2S:Er (M = Y, Gd, La) phosphor under 1550 nm excitation. Mater. Lett. **68**, 395–398 (2012). doi:10.1016/j.matlet.2011.10.087
32. H.L. Han, L.W. Yang, Y.X. Liu, Y.Y. Zhang, Q.B. Yang, Upconversion luminescence switching in Er3 + -containing ZnO nanoparticles through Li + co-doping. Opt. Mater. **31**, 338–341 (2008). doi:10.1016/j.optmat.2008.05.003